The Bioscan AN INTERNATIONAL QUARTERLY JOURNAL OF LIFE SCIENCES 21(1) 1337-1368, 2026 www.thebioscan.com

Comprehensive study of structural, functional, optical, morphological, and thermal properties of (1:1 Ratio) of glycine oxalate dihydrate crystals for photonic, optoelectronic and Nonlinear optical applications.

N. Rajasekar [1], K. Balasubramanian [2*]

[1]Research scholar (Reg.No: 22211072131006), PG and Research department of physics, The M.D.T Hindu college, Pettai, Tirunelveli-627010, Tamilnadu, India. E-mail : rs9012618@gmail.com

[2*]The Principal and the Head, PG and Research department of physics, The M.D.T Hindu college, Pettai, Tirunelveli-627010, Tamilnadu, India.

[1,2*]Affilliated by Manonmaniam Sundarnar University, Abishekapatti-627012, Tirunelveli, Tamilnadu, India.

***Corresponding author: K. Balasubramanian**

https://doi.org/10.63001/tbs.2026.v21.i01.pp1337-1368

KEYWORDS

structural, functional, optical, Thermal parameters – Broido and Kissinger methods, optoelectronics, photonics and Nonlinear optical applications.

Received on: 22-12-2025

Accepted on: 08-02-2026

Published on:

18-02-2026

ABSTRACT

In this investigation, the grown crystal comprehensively was systematically characterized by Powder X-ray diffraction, FTIR, UV - DRS, Photoluminescence (PL) studies and TG-DTA techniques. Powder XRD studies confirmed that the prepared sample crystallizes to the monoclinic system with a primitive lattice, confirming its well-ordered and stable crystalline nature. FTIR analysis revealed the existence of characteristics functional moeities, confirming the molecular integrity of the prepared material. UV-DRS spectral studies showed a lower cutoff wavelength at 320 nm , Tauc plot calculations indicate a direct bandgap of 5.72 eV, confirming its wide bandgap and additional optical parameters, including the Transmittance (%), extinction coefficient, optical conductivity, refractive index and reflectance (%), were systematically evaluated, demonstrating its potential for advanced optical applications. PL studies displayed a strong emission peak at 468 nm (2.65 ev), highlighting its potential for optoelectronic and photonics device applications. TG-DTA analysis, interpreted using both Kissinger and Broido methods, revealed the excellent heat stability of the material, suggesting its capability to withstand high-temperature processing. SEM analysis was performed to examine the surface features of the prepared material. The micrographs reveal well-defined crystalline facets, uniform grain distribution, and continuous microstructural patterns, indicating controlled nucleation and stable crystal growth. EDX studies demonstrated the existence of C, N, and O, verifying the elemental composition and compositional uniformity of the grown crystal. The third-order nonlinear optical (NLO) characteristics of the material were evaluated by the Z-scan studies. The results confirm its nonlinear optical absorption (β), nonlinear optical refractive index (n_2) and the magnitude of the third-order susceptibility.

Overall, the combined results from structural, functional, optical, morphological, and thermal analyses demonstrate that the grown material; exhibits remarkable properties, rendering it a potential material for applications in nonlinear optics, photonics, and opto electronic devices.

Introduction

Glycine oxalate dihydrate, an organic molecular crystal formed by the combination of glycine, the simplest amino acid, with oxalic acid, has garnered considerable interest recently owing to its unique structural, optical, and thermal characteristics **[1, 2]**. The crystal structure is stabilized through an extensive hydrogen-bonded network, which contributes significantly to its growth morphology, crystallinity, and overall structural integrity. Its high optical transparency, thermal stability, and photoluminescence behaviour rendeingr it well-suited canditate for applications such as nonlinear optics, photonic devices, optoelectronic components, and other advanced technological areas **[3]**. Detailed characterization of Glycine oxalate dihydrate is essential for understanding its functional behaviour. Powder X-ray diffraction studies provides precise information on crystallinity, lattice parameters, and crystal structure, while FTIR spectroscopy is employed to evaluate optical absorption and transmittance, which are critical for potential optical device applications. Thermogravimetric and differential thermal analysis (TG-DTA) offer important information on heat stability, decomposition behavior, and phase transitions, which are crucial for assessing practical usability **[4]**. The optical, morphological, and compositional characterized of the prepared sample were characterized using UV-DRS, SEM studies and EDAX techniques. The third-order nonlinear optical (NLO) characteristics were evaluated by the Z-scan studies to assess its suitability for NLO applications. Controlled crystal growth methods, including slow evaporation and solution growth, allow for the optimizing of crystal size, shape and purity, thereby improving the material's performance and expanding its promising applications in advanced photonic and optoelectronic devices **[5]**.

Synthesis of Glycine oxalate dihydrate crystals

Glycine oxalate dihydrate crystals were synthesized by employing a slow-evaporation growth method. Glycine A.R and oxalic acid dihydrate, with a (1:1) eqimolar proportion, were accurately weighed and dissolved in

deionized water to prepare a clear, homogeneous solution at room temperature. The mixture was continuously stirred for 5 hours to acheive complete dissolution and uniform mixing of the reactants. The resulting solution was filtered using whatmann filter paper to remove any insoluble particulates. The filterate was then transferred to a clean, dust-free environment and make them to undergo slowly at ambient temperature. After approximately 20 days, transparent, well-formed Glycine oxalate dihydrate crystals were obtained.

$$C_2H_5NO_2 + C_2H_2O_4.\ 2H_2O\ - C_4H_{11}NO_8$$

Fig. 1 (a) Photographic image of Glycine oxalate dihydrate single crystals

Fig. 1 (b). Molecular structure of Glycine oxalate dihydrate (1:1 molar ratio) single crystal

Results and discussion

1). XRD

The PXRD profile of the prepared glycine oxalate dihydrate crystals displayed intense and well-defined and distinct diffraction peaks, suggesting a high degree of crystalline **[6]**. The positions and relative intensities matched closely with the reported standard reference data, confirming the formation of a single-phase crystalline structure. The diffraction pattern also suggests that the crystal lattice is well-ordered, and no secondary phases or impurities were detected, demonstrating the purity and structural integrity of the prepared crystals **[7]**.

The synthesized crystals crystallize in the monoclinic structure with the space group P21/c. The refined lattice parameters are a =

15.418 A°, b = 6.970 A°, c = 10.064 A°, $\alpha = 90°$, β = 112.216°, γ = 90°, and the unit cell volume is V = 1081.59 $A^{\circ 3}$ with Z = 4. These lattice constants are in close consistency with the values previously documented in the literature **[8]**.

The P-XRD pattern of the prepared glycine oxalate dihydrate crystals exhibited sharp and distinct diffraction peaks with relative intensities of 18.239, 22.478, 24.09, 30.077, 36.999, 14.904, 21.600, 28.522, and 38.328, corresponding to the hkl planes (100), (103), (120), (040), (113), (101), (110), (031), and (200) respectively. The distinct and well-defined diffraction peaks clearly demonstrates the high crystalline quality and confirm the formation of a pure single-phase crystal system. The diffraction pattern reveals a well-ordered lattice arrangement in the absence of detectable impurity or secondary phase reflections, indicating excellent structural quality and phase purity.

The obtained diffraction peaks exhibits close aggrement with the standard JCPDS card of glycine A.R (JCPDS No. 07-0718) and oxalic acid dihydrate (JCPDS No. 04-0621), confirming the formation of a single –phase, highly crystalline glycine oxalate dihydrate. The sharpness and intensity of the peaks indicate a well-ordered crystal lattice, and no additional peaks were obtianed, suggesting the absence of impurities or secondary phases **[9, 10]**.

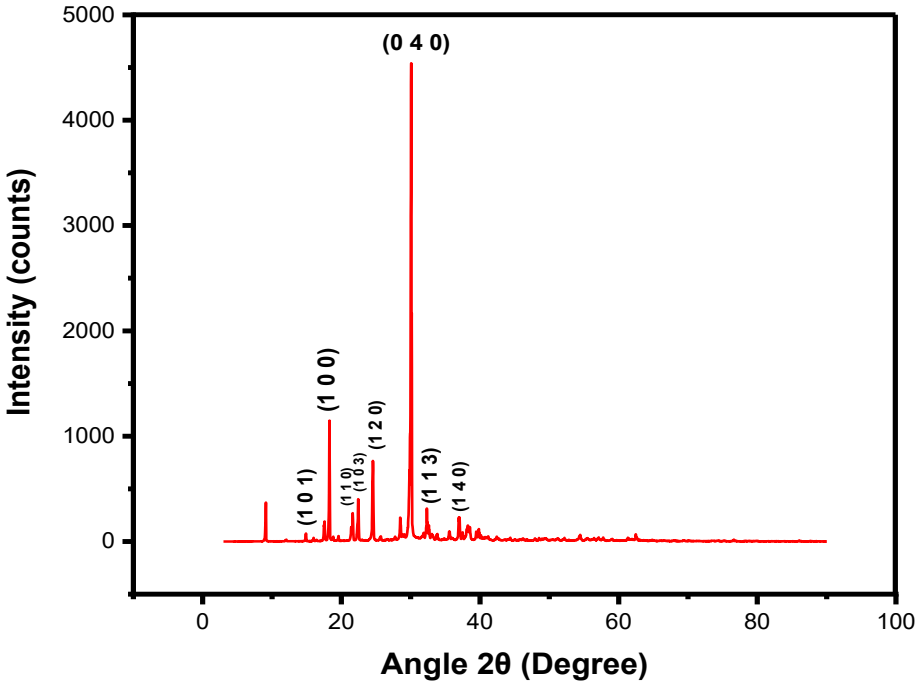

Fig 2. Shows the XRD profile of the grown crystal

2). FTIR

The spectral peak observed at 480.16 cm^{-1} is attributed to C-C bending, whereas the feature around 671.47 cm^{-1} originates from C-O bending. The absorption at 708.96 cm^{-1} is attributed to out of plane C-H bending, and the spectral peak around 890.56 cm^{-1} corresponds to C-C stretching. The feature around 1009.56 cm^{-1} is due to C-O stretching, where as the spectral peak around 1091.65 cm^{-1} arises from C-N stretching. The spectral peak around 1219.90 cm^{-1} corresponds to C-H bending and the absorption peak around 1320.45 cm^{-1} is due to COO- symmetric stretching **[11, 12]**. The spectral peak around 1429.20 cm^{-1} arises from COO- symmetric stretching, while the band around 1603.37 cm^{-1} is attributed to N-H bending. The spectral peak around 1686.16cm^{-1} and 1712.38 cm^{-1} correspond to C=O stretching of oxalate and glycine, respectively. The spectral peak around 1895.99 cm^{-1} is

attributed to C=O overtone, while the peak around 2452.12 cm^{-1} originates from O-H stretching of water. An absorption around 2852.28 cm^{-1} is due to C-H stretching, and the spectral band around 3218.53 cm^{-1} is assigned to N-H stretching, confirming the incorporation of Glycine and oxalate dihydrate moieties in crystalline structure **[13]**.

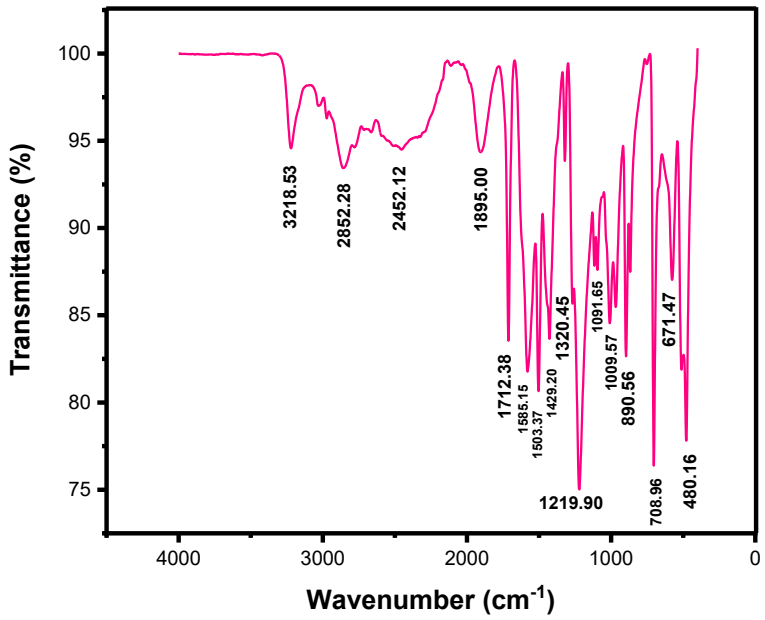

Fig. 3 FTIR graph of the synthesized Glycine oxalate dihydrate single crystal

3). UV-DRS analysis

The optical properties of the prepared material were analyzed by Ultraviolet-Diffuse reflectance spectrum (UV-DRS) to evaluate its transparency and electronic structure **[14, 15]**. The absorbance spectrum exhibits a well-defined lower cut-off at 320 nm, indicating that the material demonstrates excellent transparency across the entire visible spectral region. The pronounced absorption cutoff in the UV region arises from intrinsic electronic transitions within the molecular framework of the crystal. These transitions primarily arise from (n - σ*) and (n - π*) excitations associated with hetroatoms and functional moieties present in the material **[16].** In particular, the presence of alcohol (-OH)

groups contributes significantly to the observed electronic transitions arising from lone pair electrons on the oxygen atom, which participate in such excitations under UV irradiation **[17]**.

The transmittance spectrum exhibits a well-defined lower cutoff wavelength at 212 nm, indicating the onset of fundamental absorption in the ultraviolet region and confirming the broad optical transparency range of the material **[18].**

The optical bandgap energy was determind from the tauc plot from the diffuse reflectance data **[19]**. Extrapolation of the linear portion of $(\alpha hv)^2$ versus photon energy (hv) plot reveals a direct bandgap energy of 5.73 eV. The relatively highband gap value confirm the wide bandgap and insulating nature of the crystal. Such a large bandgap energy, combined with excellent visible region transparency, suggests that the crystal is a promising candidate for optoelectronic applications **[20, 21].**

Overall, the UV-DRS analysis demonstrates that the synthesized crystal possesses a sharp absorption edge, well-defined electronic transitions influenced by alcohol functional groups, and a wide direct bandgap, highlighting its potential for advanced optical device applications **[22]**.

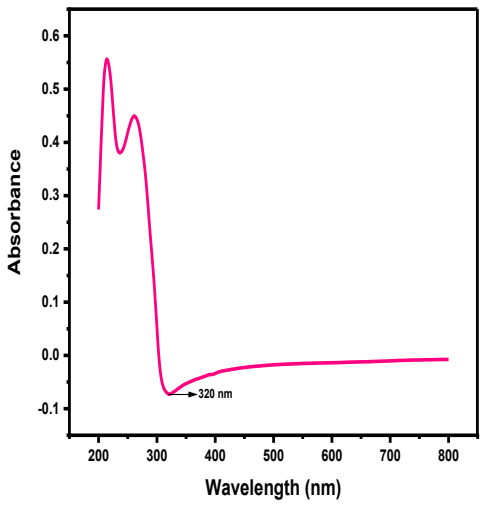

Fig.4 (a) UV DRS - Absorbance

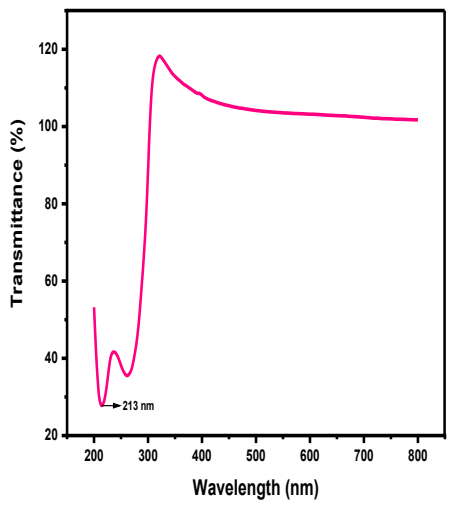

Fig. 4 (b) UV DRS - Transmittance (%)

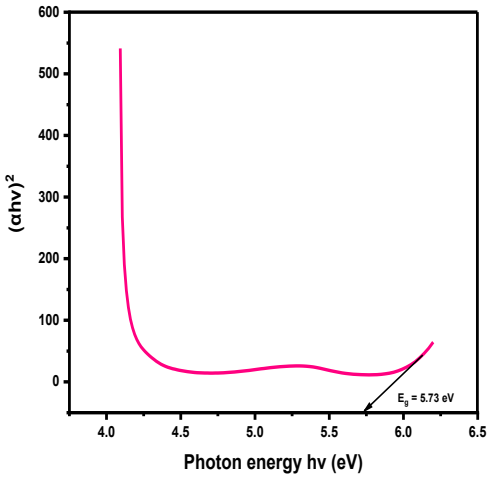

Fig. 4 (c) UV DRS – Direct bandgap energy

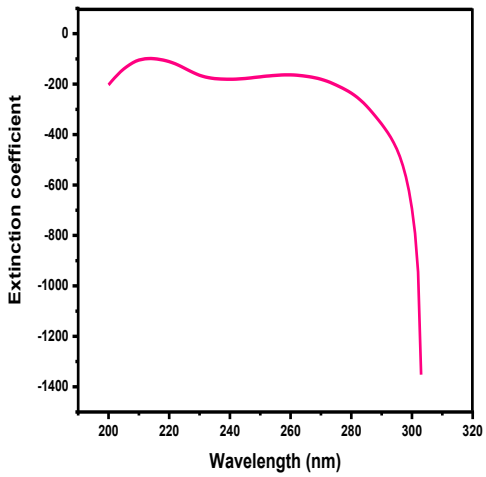

Fig. 4 (d) UV DRS - Extinction coeffecient

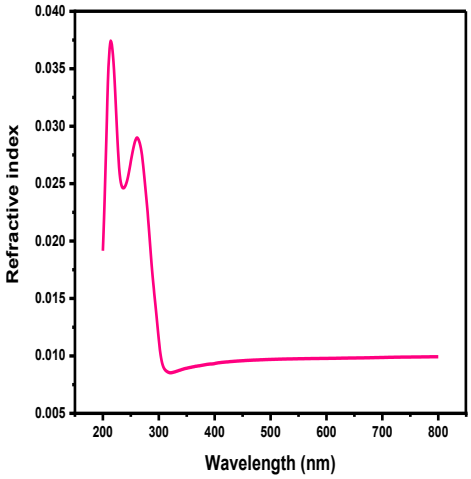

Fig. 4 (e) UV DRS - Refractive index

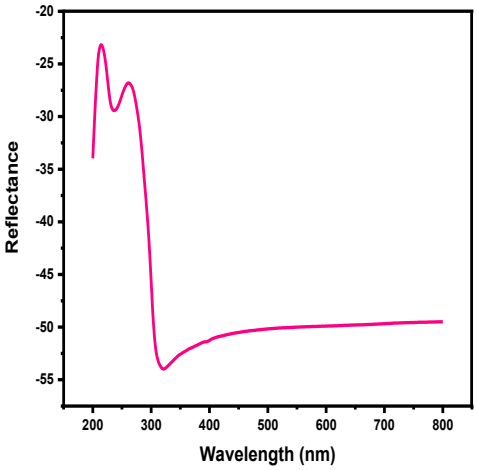

Fig. 4 (f) UV DRS - Reflectance

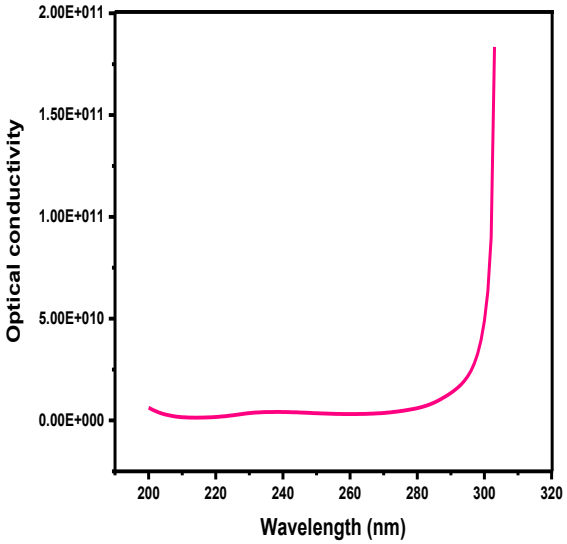

Fig. 4 (g) UV DRS - optical conductivity

4). TG DTA studies

The thermal characterization of the prepared sample were examined by thermogravimetric and differential thermal analysis (TG-DTA) **[23].** The systematic investigation was performed for a sample weighing 5.074 mg under a nitrogen atmosphere, with the heat flow recorded in the endothermic down (mw) mode **[24]**. The DTA curve displays three prominent endothermic peaks at 200.41℃, The second endothermic transition at 278.07℃ and the third endothermic peak around 407.24℃. The first endothermic transition is due to the loss of surface and lattice bound water molecules, while the second peak corresponds to the decomposition of organic functional moities in the compound **[25]**. The third transition may be related to structural rearrangement or further decomposition of the crystalline matrix, confirming the multistep thermal process of the material. The gradual nature of the decomposition process and absence of sharp exothermic peaks reveal that the compound exhibits good thermal stability **[26]**.

The TG curve shows four distinct stages of mass loss occurring the first decomposition near 181.62 ℃, the second decomposition around 250.37℃, third decomposition near

534.67 ℃ and the fourth decomposition around 689.89 ℃. The initial mass loss indicates dehydration, while subsequent losses correspond to the breakdown of the organic moieties and final degradation of carbonaceous residues **[27]**. These observation verify the existence of a well-defined crystal structure, and demonstrate that the material possesses good thermal stability **[28]**.

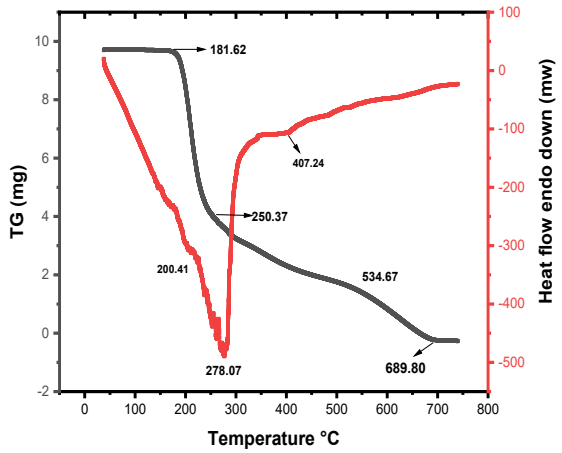

Fig. 5 (a) TG-DTA graph of the grown single crystals

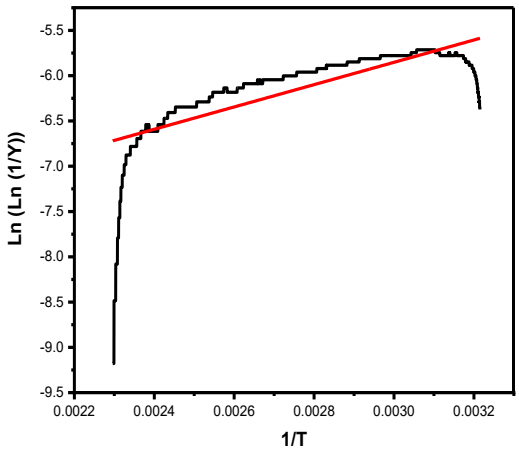

Fig. 5 (b) Broidos plot for the grown single crystal

Table. 1

Thermal parameters were calculated by the Broido method

Thermal parameters	Values
Temperature	411.52 K
Slope	1232.09147
E_a (J)	10245.2
Entropy [ΔS] (J/mol.k)	-276.1
Enthalpy [ΔH] (J/mol)	6822.6
Gibbs Free energy [ΔG] (J/mol)	120388.2

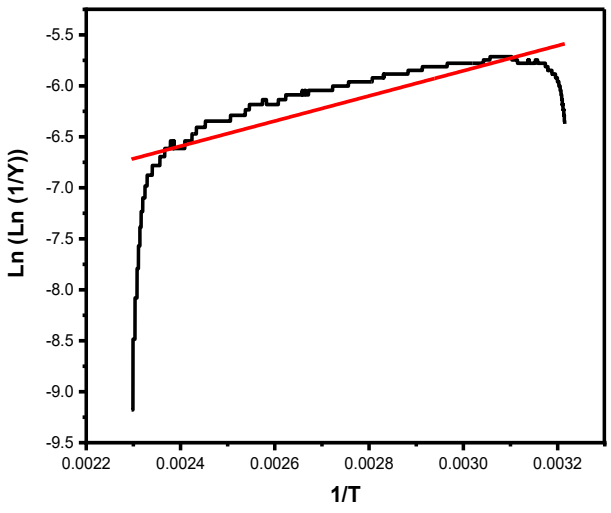

Fig. 5 (c) kissinger plot for the grown single crystal

Table. 2

Thermal parameters were evaluated through the kissinger method

Thermal parameters	Values
Temperature	487.50 K
Slope	1082.28104
E_a (J)	8993.5
Entropy [ΔS] (J/mol.k)	-285.0
Enthalpy [ΔH] (J/mol)	4938.7
Gibbs Free energy [ΔG] (J/mol)	143876.2

A comparative analysis of the thermal parameters obtained from broidos and Kissinger methods providing significant insights into the decomposition behavior of the material **[29].** Both methods confirm the excellent heat stability of the crystal, indicating its ability to withstand elevated temperatures without undergoing abrupt degradation **[30]**. The broido method, implying a more gradual and controlled breakdown process. In both approaches, the negative entropy values indicates a reduction in disorder during the decomposition, consistent with a stepwise and ordered thermal degradation mechanism **[31].** Differences in the gibbs free energy values reflect the sensitivity of the thermodynamic predictions to the analytical approach employed. Overall, the combined analysis demonstrates that the crystal exhibits a multi-step decomposition process while maintaining good thermal stability **[32].**

5). Photoluminescence

The Photoluminescences (PL) studies of the synthesized material was conducted to examine its optical and electronic characteristics, which are strongly correlated

with the structural features of the crystalline crystal **[33]**. The PL graph displayed a strong emission peak at 468 nm, located in the blue spectral region, which arises from the radioactive recombination of charge carriers within the well ordered crystalline lattice**.** This prominent blue emission indicates that the crystal possesses a high level of structural perfection and distinct electronic states **[34]**. A secondary emission band at 541 nm, located in the green region, suggests the presence of shallow defect level, which contribute to additional electronic transitions**.** Such defect-mediated emissions are typical insolution grown crystals and can influence the luminescence efficiency and tenability of the material. Furthermore, a third emission band at 823 nm was detected in the near-infrared (NIR) region, indicating the ability of the crystal to emit across a broad spectral range. This NIR emission is generally attributed to deep level transitions or impurity centers, reflecting the intrinsic and extrinsic characteristics of the material **[35]**.

The observed multi-wavelength luminescence, spanning blue region, green and NIR regions, demonstrate the versatility and broadband optical activity of the crystal **[36].** These photoluminescent properties make the material a promising candidate for optoelectronic applications, including Light emitting diodes (LEDs), Lasers and photonic devices, where controlled emission at specific wavelengths is critical **[37]**. Additionally, the NIR emission enhances its potential for bio-imaging, optical sensors, and telecommunication applications. Where near infrared luminescence is highly valued **[38]**. Therefore, the PL study not only confirms the excellent optical properties and structural integrity of the solution prepared material but also highlights its suitability for advanced technological applications in photonics and optoelectronics, establishing its significance in crystal growth research **[39].**

The photoluminescence peak at 468 nm is 2.65 eV indicates efficient electronic transitions in the grown crystal **[40]**.

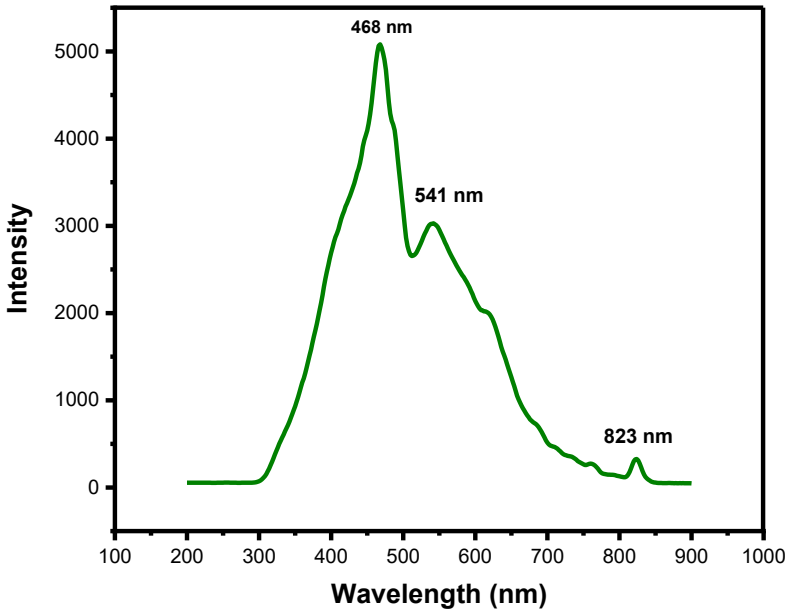

Fig. 6 PL graph of the Glycine oxalate dihydrate crystal

6). Z-Scan analysis

The third-order nonlinear optical (NLO) characteristics of the synthesized material were systematically evaluated by the standard single-beam Z-scan studies **[41]**. The investigation was performed with a continuous-wave He-Ne laser operating at 632.8 nm and an output power of 12.0 Mw. The incident laser beam, with a beam diameter of 5mm, was focused through a convex lens with a focal length 200mm to obtain a narrow beam waist at the focal region **[42]**. The crystal specimen, having a thickness of 1mm, was translated along the propagation (z-axis) over a total scanning length of 40.0 mm with an incremental step size of 0.5 mm under high-bandwidth conditions **[43]**.

An aperture of radium 2mm was positioned in the far field to carry out closed-aperture measurements, where the beam radius at the aperture was determined to be 4.5 mm. The linear refractive index (no) of the material has determined as 1.5, and linear transmittance

of the specimen was experimentally measured to be 70 %.

The Rayleigh length (Zo) of the laser beam has observed as 0.40 mm, ensuring that the sample thickness remained well within the Rayleigh range and validating the applicability of the Z-scan studies.

The third-order nonlinear optical parameters of the grown material were evaluated through employing the standard Z-scan analysis **[44].** The nonlinear refractive index (n_2) was determined as 1.33 x 10^{-16} m^2/W, indicating a measurable third-order nonlinear refractive behavior of the sample. The nonlinear absorption coefficient (β) were calculated as 3.54 x 10^{-6} m/W, confirming the presence of nonlinear absorption under laser irradiation. The real of the third-order nonlinear optical susceptibility were evaluated as 5.06 x 10^{-15} esu, and the imaginary part is evaluated to be 4.53 x 10^{-9} esu, respectively. The overall third-order susceptibility ($\chi(3)$) was calculated to be 4.53 x 10^{-9} esu, demonstrating the potential of the grown material for advanced nonlinear optical and photonic applications **[45]**.

The open-aperture Z-scan curve display a valley followed by a peak transmittance behaviour, indicating the coexistence of reverse saturable absorption (RSA) at lower intensities followed by saturable absorption (SA) at higher laser excitation, confirming the influence of high-intensity laser irradiation on the nonlinear optical behavior of the sample **[46]**.

The closed aperture Z-scan graph reveals a clear valley-to-peak profile, which corresponds to a positive nonlinear refractive index (n_2) and confirms self-focusing behaviour of the crystal under laser illumination **[47]**.

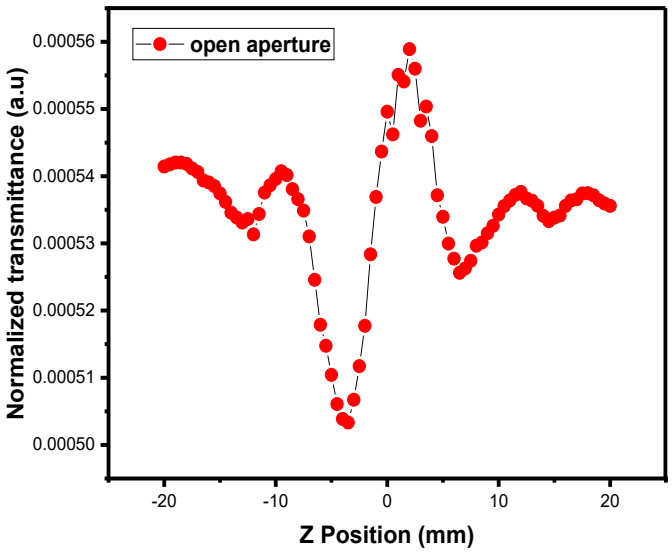

Fig. 7 (a). Open aperture in Z-scan

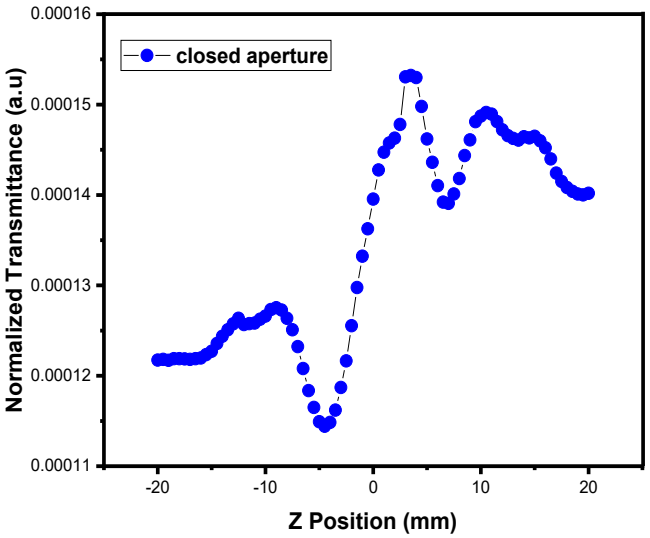

Fig. 7 (b). closed aperture in Z-scan

7). Scanning electron microscope

SEM was employed to analyze the surface features and microstructural characteristics of the grown material **[48]**. The SEM images reveal a well-defined and uniform surface morphology with closely packed grains, indicating improved crystalline order and controlled growth conditions. No prominent cracks, voids, or secondary phase formations were observed, confirming the structural stability of the crystal **[49]**. The smooth and homogeneous surface further suggests effective incorporation of the constituent molecules within the crystal lattice. Overall, the SEM analysis demonstrates that the optimized growth parameters contributed to the formation of a detect-minimized crystal with good structural integrity **[50]**.

The scanning electron microscopy (SEM) micrographs is presented in Fig. 7 (a) to Fig. 7 (e) provide a comprehensive view of the surface morphology and growth properties of the prepared material at different magnifications and regions **[51, 52]**. The images reveal well-developed crystalline features with irregularly shaped grains and clearly distinguishable growth facets, indicating anisotropic growth behaviour. A layered and interconnected microstructure is observed across the surface, suggesting a step-wise growth mechanism governed by controlled nucleation and gradual crystal propagation. Fine granular textures with localized agglomeration are visible in certain regions, which may be attributed to variations in supersaturation and solvent-solute interactions during the crystallization process **[53]**. The continuity of the surface morphology across all micrographs confirms uniform growth throughout the crystal, while the absence of major cracks or large voids indicates good structural stability. Overall, the SEM analysis demonstrates consistent microstructural evolution and confirms the formation of a well-grown crystal under optimized growth conditions **[54, 55]**.

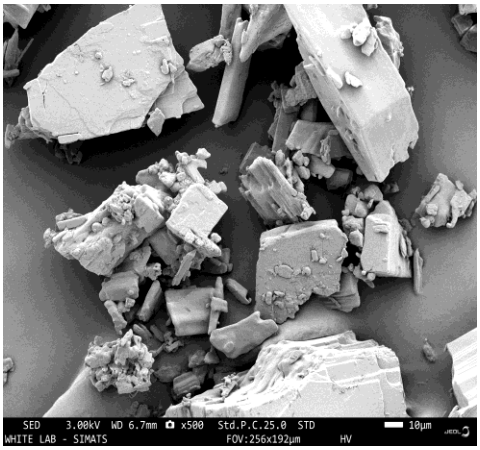

Fig. 8 (a) SEM Micrograph

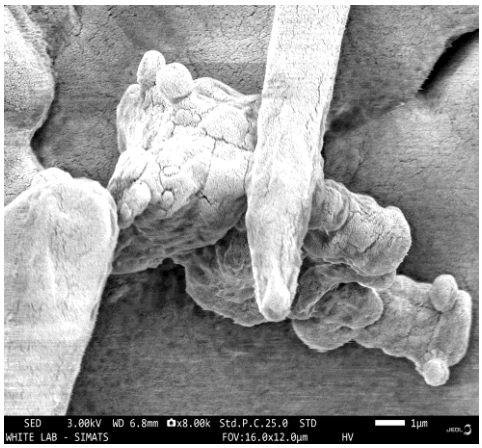

Fig. 8 (b) SEM Micrograph

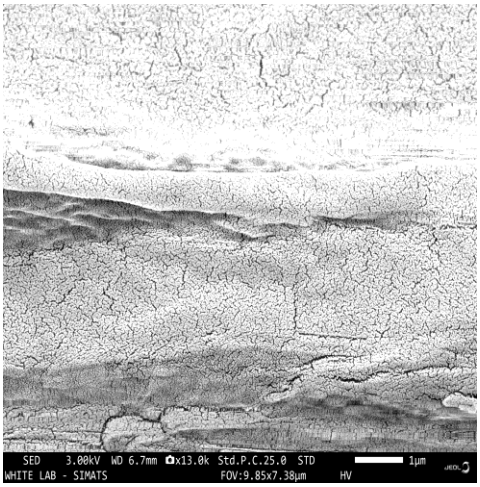

Fig. 8 (c) SEM Micrograph

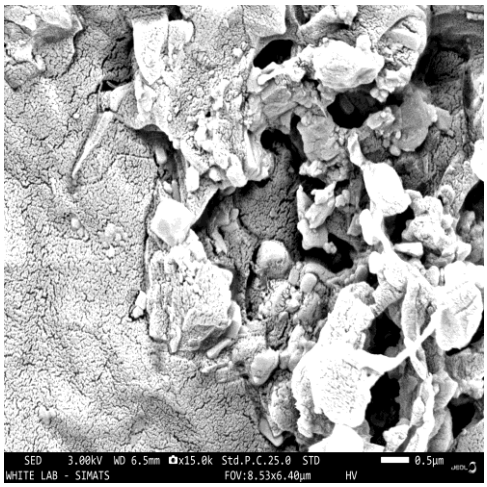

Fig. 8 (d) SEM Micrograph

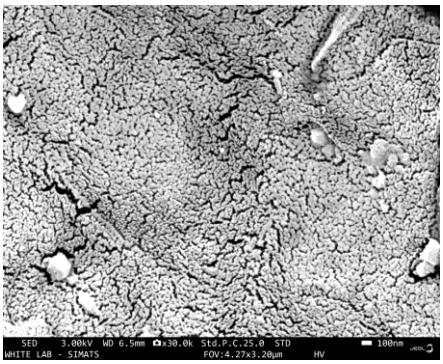

Fig. 8 (e) SEM Micrograph

8). Energy dispersive X-ray analysis

Energy dispersive X-ray spectroscopy (EDX) investigation was conducted to analyze the elemental constituent of the synthesized material **[56, 57]**. The EDX spectrum establish the confirmation of carbon, nitrogen, and Oxygen, as the major constituent elements, detected through their characteristic K-series emission lines **[58, 59]**. The observed elemental signals indicate successful incorporation of the organic molecular components within the crystal structure **[60, 61]**. The quantitative analysis reveals apparent concentrations of 71.74% for carbon, 28.78 % for nitrogen, and 25.29% for oxygen, with corresponding K-ratios of 0.71740, 0.05123, and 0.08512, respectively **[62, 63]**. The weight percentages further support the compositional uniformity of the sample, confirming the elemental purity and absence of extraneous impurity peaks within the detection limit of the instrument **[64, 65]**.

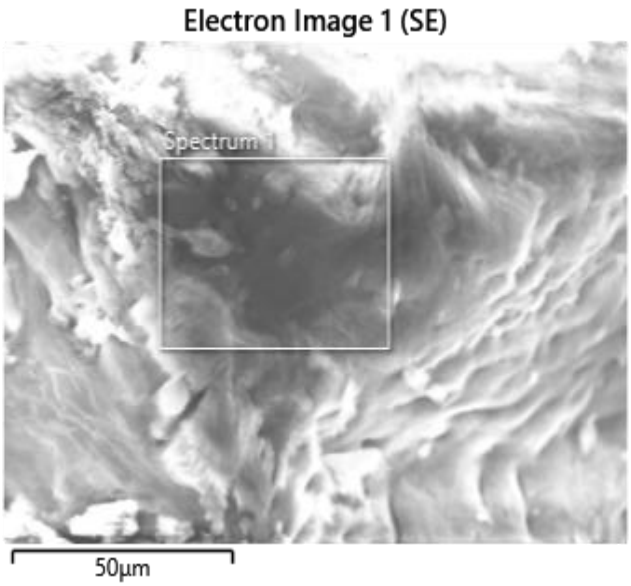

Fig. 9 (a) Electron image of EDAX spectrum

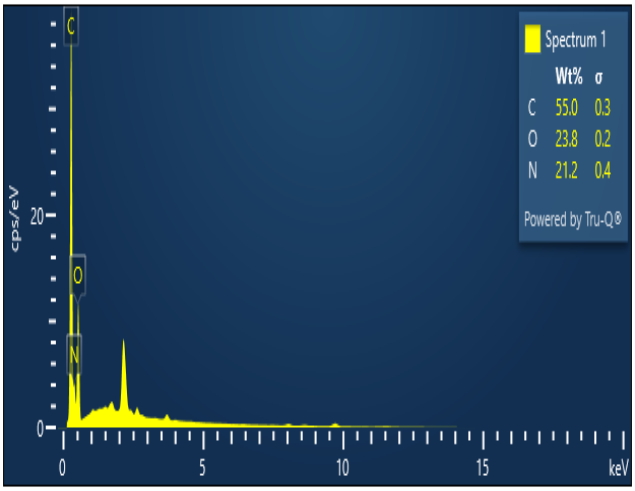

Fig. 9 (b) EDAX profile of the synthesized material

Table. 3

Elemental composition of the synthesized single crystal obtained from EDX analysis

Elements	**Signal type**	**Line**	**Apparent concentration**	**K Ratio**	**Wt%**	**Standard Name**	**Factory standard**
C	EDS	K series	71.74	0.71740	0.32	C Vit	yes
N	EDS	K series	28.78	0.05123	0.42	BN	yes
O	EDS	K series	25.29	0.08512	0.19	SiO2	yes
Total				**100.00**			

Conclusion

The prepared material was systematically successfully investigated by the Powder XRD, FTIR, UV-DRS, EDAX, SEM, photoluminescence ,TG-DTA and Z-scan techniques. XRD analysis confirmed a monoclinic crystal system with a primitive

lattice, indicating a well-ordered structure. FTIR spectra revealed various functional moieties, supporting the molecular framework of the synthesized material. The UV-DRS analysis reveals a sharp absorption lower cutoff at 320nm with high optical transmittance across the visible spectrum. The obtained bandgap energy of 5.73 eV confirms the wide bandgap and insulating behavior of the material. The plotted graph of refractive index, reflectance, extinction coefficient, along with optical conductivity further indicate low optical loss and good dielectric behaviour, suggesting the crystal is applicable for optoelectronic applications. Photoluminescence (PL) studies exhibited a maximum emission peak at 468 nm (2.65 eV), highlighting its suitability for optoelectronic and photonic device applications. TG-DTA studies supported by both Kissinger and broidos methods, confirmed the excellent heat stability of the crystal. The Z-scan results reveal a nonlinear optical absorption coefficient (β) of 3.54 x 10^{-6} m/W and a nonlinear optical refractive index (n_2) of 1.33 x 10^{-16} m^2/W, yielding a third-order nonlinear optical susceptibility $\chi^{(3)}$ of 4.53 x 10^{-9} esu, which confirms the material's appreciable third order nonlinear optical behavior. Overall, the comprehensive characterization reveals that the material exhibits superior structural, optical and thermal properties, making it applicable for photonics and opto electronic device applications. The SEM analysis confirms uniform surface morphology and consistent microstructural evolution across the crystal, indicating controlled nucleation and stable growth throughout the crystallization process. The EDX study confirms that carbon (C), nitrogen (N), and oxygen (O) are the major atomic constituent of the grown crystal, demonstrating its uniform elemental composition and structural integrity.

References

[1]. N. Rajasekar, K. Balasubramanian. Crystallization and multifaceted characterization of L-Asparagine monohydrate single crystals for structural, spectroscopic, Optical, Thermal and morphological analysis toward for Third order NLO applications. International Journal of Applied Mathematics. Volume 38, No. 10s, (2025). ISSN: 1311-1728 (printed version); ISSN: 1314-8060 (on-line version)

DOI : https://doi.org/10.12732/ijam.v38i10s.992

[2]. N. Rajasekar, K. Balasubramanian. Advanced growth and multifunctional characterization of L-Threonine single crystals: comprehensive Insights for structural, Functional, optical, Mechanical, Antibacterial and Thermal properties with potential in optoelectronics, Photonics and nonlinear optical applications. The bioscan an international quarterly journal of life science (www.thebioscan.com). 21(1): 685-731, (2026). ISSN: 0973-7049 (P).

DOI: 10.63001/tbs.2026.v21.i01.pp685-731

[3]. R. Priya, S. Krishnan, C. Justin Raj, and S. Jerome Das. Growth and characterization of NLO active lithium sulphate monohydrate single crystals. Cryst. Res. Technol. 44, No. 12, 1272 – 1276, (2009).

DOI : 10.1002/crat.200900504

[4]. J. Suja Rani , K. Jaya Kumari and C. K. Mahadevan. Thermal, electrical and photoconductivity properties of L-leucine hydrobromide (LEHBr): A semiorganic nonlinear optical single crystal. Archives of Applied Science Research, 2013, 5 (4):127-136

[5]. B. Ravindran , S. Malini , N. Menaka , S. Ambikavathy, S. Kamali. Growth and characterization of a new nonlinear optical material L-Leucine thiourea crystal. Journal of Emerging Technologies and Innovative Research (JETIR) (www.jetir.org). (2018), July 2018, Volume 5, Issue 7, (ISSN-2349-5162)

[6]. Gershom Jebaraj .P, Sivashankar .V. Crystal growth in solution and characterization of Rubidium sulphate single crystals doped with L-Leucine. Journal of Advanced Scientific Research. (2022), 13 (6), 60-68.

DOI : https://doi.org/10.55218/JASR.202213610

[7]. S. Arul mani, and S. Senthil. Growth and optical studies on L-Leucine doped ADP single crystals for nonlinear optical applications. Materials today: proceedings. 5, (2018), 8996-9003.

[8]. M. Malar wezhli, G. Suresh, G. Srinivasan, R. Sumalatha, R. Manickam. Investigation on synthesis, growth and characterization of glycine oxalate dihydrate:

A new semiorganic nonlinear crystal for optical applications. Optik. (2016).

DOI : http://dx.doi.org/10.1016/j.ijleo.2016.01.187

[9]. M. Arul Tresa , B. Helina , S. C. Vella Durai. Investigations on the Growth and Optical, Dielectric and Antibacterial Activity of L-leucine Barium Chloride Crystals. Eurasian Journal of physics and functional materials. Volume 8, Number 3, Page- 122-130

[10]. Jagadeesh M. R, Suresh kumar. H. M, Ananda kumar. R. Growth and characterization of NLO crystal : L-leucine phthalic acid potassium iodide. Materials Science-Poland, 33(3), 2015, pp. 529-536

DOI : 10.1515/msp-2015-0063

[11]. A. Venkatesan, S. Arulmani, S. Senthil, M.E. Rajasaravanan. Growth and Characterization of L-Leucine Doped Ammonium Dihydrogen Phosphate (ADP) Single Crystal A Nonlinear Optical Application. (2019), Materials Today: Proceedings, PP. 148-152.

DOI : 10.1016/j.matpr.2019.02.093

[12]. G. Bhagavannarayana, B. Riscob, Mohd. Shakir. Growth and characterization of l-leucine l-leucinium picrate single crystal: A new nonlinear optical material. Materials Chemistry and Physics 126, (2011), 20-23.

DOI : 10.1016/j.matchemphys.2010.12.040

[13]. R. Omegala Priakumari, S. Grace Sahaya Sheba, and M. Gunasekaran. Growth and characterization of semi-organic nonlinear optical crystals of L-leucine hydrochlorobromide (LEHCBr). Can. J. Phys. 93: 836–840, (2015)

DOI : dx.doi.org/10.1139/cjp-2014-0521

[14]. V. Mohanraj, S.S. Elango, S. Ponnusamy. Growth, optical, spectral, thermal and mechanical investigations of organic NLO crystal cis-2, 6-bis(4-chlorophenyl)-3, 3dimethylpiperidin-4-one. Bulletin of scientific research. Vol 3, Iss 1, Year 2021

DOI: https://doi.org/10.34256/bsr2112

[15]. S. Vetrivel, R. Rajasekaran, K. Kanagasabapathy, S. Gopinath, Suman bhattacharya. Growth and characterization of zinc doped l-proline cadmium chloride monohydrate single crystals for non linear

optical applications and UV sensors. Opto electronics and Advanced materials – Rapid communications. Vol. 6, No. 5-6, (May - June 2012)

[16]. P. Sathya, M. Anantharaja, N. Elavarasu, and R. Gopalakrishnan. Growth and characterization of nonlinear optical single crystals: bis(cyclohexylammonium) terephthalate and cyclohexylammonium para-methoxy benzoate. Bull. Mater. Sci, Vol. 38, No. 5, September 2015, pp. 1291–1299.

[17]. M. Suresh, S. Asath Bahadur and S. Athimoolam. Crystal growth and characterization of a new NLO material: 4-Methoxyaniline. Advances in Applied Science Research, (2013), 4(4):160-164.

[18]. R. Purusothaman, M. Shankar, A. Dennis Raj, M. Vimalan, and I. Vetha Potheher. A study on NLO, ultraviolet transparency, photoconductivity, and dielectric response of organic single crystal. J Mater Sci: Mater Electron. (2023), 34:2292.

DOI : https://doi.org/10.1007/s10854-023-11691-1

[19]. J. Madhavan, S. Aruna, K. Prabha, J. Packiam julius, Ginson. P. Joseph, S. Selvakumar, P. Sagayaraj. Growth and characterization of a novel NLO crystal L-Histidine hydrofluoride dihydrate (LHHF). Journal of crystal growth. 293, (2006), 409-416.

DOI : 10.1016/j.jcrysgro.2006.05.050

[20]. Christy. D, Sahaya Shajan X and Mahadevan C. K. Study of Physico-Chemical Properties and Growth Dimension Augmentation of Barium Succinate Single Crystals Grown by Slow Evaporation Technique. Journal of Physical Science, Vol. 33(1), 29–49, 2022.

[21]. Gershom Jebaraj .P, Sivashankar .V. Crystal growth in solution and characterization of Rubidium sulphate single crystals doped with L-Leucine. Journal of Advanced Scientific Research. (2022), 13 (6), 60-68.

DOI : https://doi.org/10.55218/JASR.202213610

[22]. A. Senthil , T. Bharanidharan, M. Vennila, Elangovan K, S. Muthu. Crystal growth, Hirshfeld analysis, optical, thermal, mechanical, and third-order non-linear optical

properties of Cyclohexylammonium picrate (CHAP) single crystal. Heliyon 10 (2024) e28002.

DOI : https://doi.org/10.1016/j.heliyon.2024.e28002

[23]. S. Dhanushkodi, S. Manivannan, J. Philip. Growth, structural, thermal, and optical properties of organic NLO crystal. N-Methyllutidone trihydrate. Journal of crystal growth 265, (2004), 284-289.

DOI : doi:10.1016/j.jcrysgro.2004.01.060

[24]. M. Esthaku Peter, P. Ramasamy. Structural, growth and characterizations of NLO crystal: Triglycinium calcium nitrate. Adv. Mater. Lett. (2016), 7(1), 83-88.

[25]. Radhakrishnan Lakshmi, Peethambaram Prabukanthan, Gurusamy Harichandran, and C. Sudarsana Kumar. Synthesis, Crystal Growth, and Optical Characterization of a Novel Nonlinear Optical Organic Material: N,N-Diarylbenzamide. Cryst. Res. Technol. (2018), 1700146.

DOI: 10.1002/crat.201700146

[26]. V.S. Dhanya, M.R. Sudarsanakumar, S. Suma, S. Prasanna, K. Rajendra Babu, B. Suresh Kumar, Sunalya M. Roy. Growth and characterization of a new polymorph of lead succinate: A promising NLO material. Journal of Crystal Growth. 319, (2011), 96–101.

DOI : 10.1016/j.jcrysgro.2011.01.073

[27]. M. Parthasarathy, R. Gopalakrishnan. Growth and characterization of methyl 2-amino-5-bromobenzoate crystal for NLO applications. Spectrochimica Acta Part A: Molecular and Biomolecular Spectroscopy. 97, (2012), 1152-1158.

DOI : http://dx.doi.org/10.1016/j.saa.2012.07.132

[28]. A. Puhal Raj, C. Ramachandra Raja. Synthesis, Growth, Structural, Spectroscopic, Thermal and Optical Properties of NLO Single Crystal: L-Threonine Zinc Acetate. Photonics and Optoelectronics (P&O). Volume 2, Issue 3, July (2013).

[29]. M. Prakasha, D. Geetha, M. Lydia Caroline. Synthesis, structural, optical, thermal and dielectric studies on new organic nonlinear optical crystal by solution growth technique. Spectrochimica Acta Part A: Molecular and

Biomolecular Spectroscopy. 107, (2013), 16–23.

DOI : http://dx.doi.org/10.1016/j.saa.2013.01.012

[30]. A Hemalatha, S Arulmani, P Sanjay, K Deepa, J Madhavan and S. Senthil. Growth and Characterization of L-Leucenium Hydrogen Maleate Single Crystals for Nonlinear Optical Applications. IOP Conf. Series: Materials Science and Engineering. 360, (2018), 012044.

DOI : 10.1088/1757-899X/360/1/012044

[31]. B. A. Shingade, R. M. Belekar, P. S. Sawadh, K. G. Rewatkar. XRD, FTIR, TGA, EDX, Investigations of L-Leucine doped in ammonium dihydrogen phosphate (ADP) single crystal. International journal of current engineering and scientific research (IJCESR). Volume - 6, Iuuse - 1, (2019). . ISSN (PRINT): 2393-8374, (ONLINE): 2394-0697.

[32]. I. Shubashini, S. R. Jebas. Growth, Spectral, Electrical, Photoluminescence, Thermal, Mechanical and Dielectric Studies of 2-Hydroxy Benzoic Acid (Metabolite of Drug Aspirin) Single Crystal. J. Sci. Res. 17 (1), 211-225, (2025).

[33]. Fredselin R. S Vithel, R. Manimekalai. Growth and characterization of L-Phenyl alanine added sulphamic acid single crystals. Journal of Advanced Scientific Research. 2021; 12 (2), Suppl 1: 145-152

[34]. Shobha Kulshrestha, A.K. Shrivastava. Crystal Growth, Optical and Structural Properties of MNA Doped L-Histidine Single Crystal. Archives of Physics Research, (2016), 7(3):9-17.

[35]. P. Anandan, S. Vetrivel, R. Jeyavel, C. Vedhi, G. Ravi, G. Bagayanarayana. Crystal growth, structural, and photoluminescence studies L-Tyrosine hydrobromide semi organic single crystal. Journal of physics and chemistry of solids. 73, (2012), 1296-1301.

DOI : http://dx.doi.org/10.1016/j.jpcs.2012.06.015

[36]. M. Parthasarathy. Optical, Photoluminescence and Second Harmonic Generation of new Organic Crystal and its Characterization. Journal of Emerging Technologies and Innovative Research (JETIR) . December 2018, Volume 5, Issue 12. (ISSN-2349-5162)

[37]. M. Nithya, M. Anbu Arasi, M.Alagar. Development of Nonlinear Optical (NLO) Crystal LPhenylalanine Doped Ammonium Dihydrogen Ortho Phosphate (ADOP). Journal of Emerging Technologies and Innovative Research (JETIR) www.jetir.org. (March 2019), Volume 6, Issue 3. (ISSN-2349-5162)

[38]. A. Silambarasan, P. Rajesh, and P. Ramasamy. Crystal Growth, Optical and Thermal Studies of 4-Nitroaniline 4Aminobenzoic Acid: A Fluorescent Material. Chemical Science Review and Letters. (2014), 2(6), 521-525. ISSN 2278-6783

[39]. P. Lalitha, S. Arumugam, A. Sinthiya, C. Nivetha, M. Muthuselvam. Oxalic acid incorporated acetamide single crystal growth dynamics, characterization, NLO and antimicrobial activities via shock wave treatment. Results in Chemistry. 5, (2023), 100790,

DOI : https://doi.org/10.1016/j.rechem.2023.100790

[40]. S. Sindhusha, C. M. Padma, B. Gunasekaran, H. Marshan Robert. Structural, optical, thermal analysis of creatininium borate – A new semiorganic NLO single crystal. Journal of molecular structure. 1209, (2020), 127981.

DOI : https://doi.org/10.1016/j.molstruc.2020.127981

[41]. B. Thirumalaiselvam, R. Kanagadurai, D. Jayaraman, V. Natarajan. Growth, XRD, Optical absorption spectrum, FTIR Spectroscopy and Z – scan study of L- Serine. International Journal of ChemTech Research. CODEN (USA): (IJCRGG). Vol.8, No.08, pp : 363-370, (2014-2015). (ISSN: 0974-4290).

[42]. S. Priya, T. Umadevi, S. Gowri, G. Vinitha. Crystal growth, structural, spectral, optical, DFT analysis and Z-scan analysis of pyridine-1-ium-2-carboxylatehydrogenbromide (PHBr) for optoelectronic and nonlinear optical applications. Journal of the Indian Chemical Society. 99, (2022), 100397.

DOI : https://doi.org/10.1016/j.jics.2022.100397

[43]. T. Tilak, M. Baseer ahamed, G. Marudhu, G. Vinitha. Effect of KDP on the growth, thermal, and optical properties of L-

Alanine single crystals. Arabian Journal of Chemistry. (2016), 9, 676–680

DOI : http://dx.doi.org/10.1016/j.arabjc.2013.04.022

[44]. T. Manju, and P. Selvarajan. Investigations on Growth and Characterization of Mono-Urea Oxalic Acid Crystals. International Journal of Applied Engineering Research. Volume 13, Number 13m (2018), pp. 11054-11061. (ISSN 0973-4562).

[45]. T. Sivanesan, V. Natarajan, D. Jayaraman, and S. Pandi. Third order Non-Linear optical properties of Vanillin Single Crystals by Z-Scan Technique. Archives of Physics Research, 2014, 5 (4):16-21.

[46]. K. J. Arun, S. Jeyalakshmi. Growth and characterization of glycinium oxalate crystals for nonlinear optical applications. Optoelectronic and advanced material – Rapid communications. Vol. 2, No. 11, November 2008, p. 701 – 706.

[47]. K. Thilaga, P. Selvarajan, S.M. Abdul Kader. Growth, Surface Morphology and Mechanical Properties of Potassium Hydrogen Sulphate Single Crystals for Antimicrobial and Third-Order NLO Applications. Physics and chemistry of solid state. V. 24, No. 4, (2023, pp. 774-779.

DOI: 10.15330/pcss.24.4.774-779

[48]. G. Ramasamy, and J. Anandakumaran. Crystal growth, structure, and characterization of Tutton's salt mixed crystals – Pottasium magnesium manganese sulphate hexahydrate. International journal of research pharmacy and chemistry. IJRPC (2020), 10(1), 54-62. (ISSN: 2231-2781)

[49]. B. Neelakantaprasad, G. Rajarajan, T. Jayanalina, D. Marimuthu, J. Senthikumar, C. Sadeeshkumar, and A. Jegatheesan. An investigations of SEM, Dielectric, and NLO properties of Thiourea potassium chloride (TPC) single crystals. Vol. 7 | No.3 |269 – 272 | July – September | 2014 ISSN: 0974-1496 | e-ISSN: 0976-0083.

[50]. Tariq Mustafa, Bindu Raina, Harjinder singh, Yaseen ahmed, and K. K. Bamzai. Crystal growth, structure, morphology, optical, thermal and electrical studies of dysprosium chloride–thiourea semi-organic complex crystal. Pramana – J. Phys. (2023), 97:139.

DOI : https://doi.org/10.1007/s12043-023-02615-z

[51]. N. Senthilvelan, G. Rajarajan, S. Sivakumar, J. Elanchezhiyan and A. Jegatheesan. Bulk growth and physical properties of Nonlinear optical material : Thiourea sulphamic acid crystal. Rasayan J. Chem., 10(1), 245 -253, (2017).

DOI : http://dx.doi.org/10.7324/RJC.2017.1011566

[52]. Berlin Beno T L, M Maria Lenin and Abina Shiny R S. Synthesis and Characterization of Semi-Organic Sodium Thiocyanate Potassium Sulphate (STPS) Crystal using Slow Evaporation Method. Indian Journal of Pure & Applied Physics Vol. 63, March 2025, pp. 240-254

DOI : 10.56042/ijpap.v63i3.15628

[53]. A. N. Prabhu, A. Jeyarama, K. Subramanya bhat, V. Upadhyaya. Growth, characterization, and structural investigations of a novel nonlinear optical crystal. Journal of Molecular Structure. 1031, (2013), 79-84.

DOI : http://dx.doi.org/10.1016/j.molstruc.2012.06.057

[54]. P. Aruna, N. Lavanya, B. Ravindran, A. Rakini, C.K. Nithya. Crystal Growth and Characterization of Nickel (II) Cinnamaldehyde Sulfate Optical Crystal by Slow Evaporation Method. Nanotechnology Perceptions (www.nano-ntp.com). 20, No.7, (2024), 3044-3057. (ISSN 1660-6795).

[55]. P. Revathi, T. Balakrishnan, J. Thirupathy. An Investigation on Structural, Optical, Thermal, and Dielectric Analysis of L-Lysine Iodide Semiorganic Nonlinear Optical Single Crystal for Opto-electronic Application. Brazilian Journal of Physics. (2024). 54 : 209

DOI : https://doi.org/10.1007/s13538-024-01588-7

[56]. Paul M Dinakaran and S.Kalainathan. Nucleation Kinetics, Chemical Etching, Sem, Edax And Mechanical Studies Of 3-Methyl 4-Methoxy 4-Nitrostilbene (MMONS): A Potential Nonlinear Optical Crystal. International Journal of ChemTech Research CODEN (USA) : (IJCRGG), Vol.5, No.1, pp

262-270, (Jan - Mar2013). (ISSN : 0974-4290).

[57]. S. J. Nandre, S.J. Shitole, R.R. Ahire. Study of Growth, EDAX, Optical properties and Surface Morphology of Zinc Tartrate Crystals. Journal of Nano and electronic physics. Vol. 4, No 4, 04013, (4pp), (2012).

[58]. M. Selvapandiyana, S. Sudhakar, M. Prasath. Growth and Physical Properties of Pure and Potassium Iodide Doped Zinc Tris Thiourea Sulphate Single Crystals. Int. Journal of Engineering Research and Application (www.ijera.com). Vol. 7, Issue 8, (Part -3) August 2017, pp.65-72. ISSN : 2248-9622

[59]. V. Vasantha Kumari, P. Selvarajan, and R. Thilagavathi. Growth and characterization of L-proline potassium bromide: A semiorganic NLO crystal. Journal of Chemical and Pharmaceutical Research, 2015, 7(9):133-143. (ISSN : 0975-7384).

[60]. S. J. Nandre, S. J. Shitole, R. R. Ahire. Study of growth, EDAX, optical properties and surface morphology of zinc Tartrate crystals. Journal of Nano and electronic physics. Vol. 4, No. 4, 04013 (4pp), (2012).

[61]. M. Meena, M. Shalini, B. Samuel Ebinezer, R. S. Sundararajan, T. C. Sbari girisun, and E. Manikandan. Investigation on crystal growth, spectral, linear optical studies, and third-order nonlinear optical analysis of L-Cysteine hydrochloride monohydrate lithium sulphate (L-CHMLS) single crystals for optical limiting applications. J Mater Sci : Mater Electrons. (2023), 34 : 1778.

DOI : https://doi.org/10.1007/s10854-023-11195-y

[62]. S. Sudha, C. Rathika Thaya Kumari, M. Nageshwari, P. Ramesh, G. Vinitha, M. Lydia caroline, G. Mathubala, A. Manikandan. Crystal growth, optical, spectroscopic studies, PL Behaviour and Hirshfield surface analysis of a third-order nonlinear optical cesium hydrogen oxalate Dihydrate (CHOD) single crystal. Journal of materials science : Materials in electronics

DOI : https://doi.org/10.1007/s10854-020-04066-3

[63]. N. Rajasekar, K. Balasubaramanian. Exploring structural, spectroscopic, Optical, Morphological, Mechanical, Antibacterial and Thermal parameters of Glycine A.R single

crystals for advanced opto electronics, Photonics, Laser components and Nonlinear optical applications. Journal of nanotechnology perceptions (www.nano-ntp.com). 20 No. S 14 (2024), 4857-4893. ISSN 1660-6795.

DOI : https://doi.org/10.62441/nano-ntp.vi.5784

[60]. N. Rajasekar, K. Balasubramanian. Design and evaluation of structural, spectroscopic, optical, thermal, morphological, and mechanical properties of L-alanine admixtured with oxalic acid dihydrate(1:1 ratio) single crystals for advanced optoelectronic, photonic, laser, and nonlinear optical applications. Journal of applied Bioanalysis. Vol. 11, No.6s, p. 1070-1093, December (2025). (ISSN 2405-710X)

DOI:

http://doi.org/ 10.53555/jab.v11si6.2526

[65]. N. Rajasekar, K. Balasubramanian. Physiochemical and multitechnique characterization of structural, functional, optical, Thermal, Microbiological, Elemental, mechanical and Antibacterial properties of L-Asparagine monohydrate admixtured with Oxalic acid dihydrate with a focus on nonlinear optical applications. The bioscan An international quarterly journal of life sciences (www.thebioscan.com). 21 (1), 1087-1125, (2026).

DOI : https://doi.org/10.63001/tbs.2026.v21.i01.pp1087-1125